Numerical investigation of an add-on thrust vector control kit

Mohamed G. AbuElkhier[1a], Sameh Shaaban[1b] and Mahmoud Y.M. Ahmed[*2]

*[1]Mechanical Engineering Department, College of Engineering and Technology-Cairo Campus,
Arab Academy for Science, Technology and Maritime Transport (AASTMT), Cairo, Egypt*
[2]Aerospace Engineering Department, Military Technical College, Cairo, Egypt

Abstract. Instead of developing new guided missiles, converting unguided missile into guided ones by adding guidance and control kits has become a global trend. Of the most efficient and widely used thrust vector control (TVC) techniques in rocketry is the jet vanes placed inside the nozzle divergent section. Upon deflecting them, lift created on the vanes is transferred to the rocket generating the desired control moment. The present study examines the concept of using an add-on jet vane TVC kit to a plain nozzle. The impact of adding the kit with different vanes locations and deflection angles is numerically investigated by simulating the flow through the nozzle with the kit. Two hinge locations are examined namely, at 24% and 36% of nozzle exit diameter. For each location, angles of deflection namely 0°, 5°, 10°, and 15° are examined. Focus is made on variation of control force, thrust losses, lift and drag on vanes, jet inclination, and jet flow structure with TVC kit design parameters.

Keywords: add-on kit; CFD; jet vanes; Nozzle flow; Thrust vector control

1. Introduction

Out of the two systems of vehicle flight control namely, aerodynamic and thrust vector control (TVC), the latter has many relative advantages. TVC provides higher vehicle response and maneuverability and is suitable for heavy and slowly moving vehicles. It can also extend the vehicle performance envelope by operating in the post-stall regime and in high-altitude flights. In addition, TVC enables minimizing the need for large aerodynamic control surfaces and the associated actuation mechanisms and drag penalty. This has the effect of reducing drag and weight (and hence increasing the range) and radar cross section (and hence increasing the survivability) of the vehicle (Danielson and Dillinger 1989, Hunter and Deere 1999). However, TVC may not completely replace aerodynamic control solutions. In fact, in cases where extremely high maneuvers are needed, both systems may act simultaneously.

Apart from using separate thrusters for control, TVC systems can be categorized into moveable and fixed nozzle systems (Tekin *et al.* 2010). The first type requires special materials and complicated technologies but is considered as loss-free system (Nauparac *et al.* 2015). In the other type, additional components are introduced to the fixed nozzle design to redirect the jet generated by the nozzle thus achieving the TVC functionality. Losses in the thrust are the penalty for the

---

*Corresponding author, Associate Professor, E-mail: mahmoud.yehia@mtc.edu.eg

relative simplicity of this TVC system. Fixed nozzle TVC systems include mechanical systems and secondary fluid injection systems (Tekin *et al.* 2010). Mechanical systems generally rely on some kind of mechanical obstacle that is used to change the thrust direction (Davidović *et al.* 2015). Several mechanical TVC systems have been developed including jet vanes, jetavators, internal maneuvering vanes, axial, domed, and segmented domed deflectors, and spoilers. (Branislav *et al.* 1987) presented an overview for their theoretical and experimental investigations on design features of mechanical TVC system. To select the most promising TVC systems, (Fuentes and Thirikill 1964) developed a selection method for preliminary design purposes.

In the recent years, a new approach in missile control system implementation has emerged. In this approach, self-contained add-on kits are developed and attached to the unguided missile. Such kits would provide unguided missiles with control capabilities turning them into guided ones in a cost-effective way compared with developing new guided missiles (BAE 2018). In many practical cases, modifying the design of an existing nozzle module to incorporate a TVC is economically and technologically unattainable. In such cases, an add-on mechanical fixed-nozzle TVC kit is sought. In cases where TVC is only used for a short interval of flight (as in turn maneuvers), a disposable TVC kit may be recommended to minimize thrust losses in subsequent flight phases.

Compared with other mechanical fixed-nozzle TVC techniques, jet vane TVC has many relative advantages. They include low actuation force and quick response (Davidović *et al.* 2015), simple and compact design (Loyd and Thorp 1978), simple and low-cost manufacturing (Facciano *et al.* 2002), and the capability of roll control for minimum vehicle alignment time. The main drawback of jet-vane TVC is the existence of thrust losses even with no vane deflection (Söğütcü and Sümer 2019, Kostic 2017). More importantly, jet vanes have the additional advantage of being more synergic as far as a disposable add-on TVC kit is concerned. Facciano *et al.* (2002) conducted experimental tests on a disposable add-on jet vane TVC kit for Sea Sparrow missile to achieve boost phase maneuvering following shipboard vertical launch.

In jet vane mechanical TVC, vanes (which design is generally similar to that of a supersonic wing (Yu *et al.* 2004a)) are installed at the rear of the rocket nozzle. Upon deflecting them, the lift generated on the vanes is transmitted to the carrying vehicle yielding the control moment. In addition, a lateral force is generated by the deflected jet. The aspects of jet vane TVC have been investigated widely in many studies; the majority of which focused on thermal stresses and erosion issues impacting the jet vanes. Yu *et al.* (2004a, 2004b, 2006) conducted a series of studies on jet vanes using simulation techniques. They defined the surface temperature, thermal stresses, and surface ablation rate distributions along the vanes. Similarly, Rahaim *et al.* (1996) and Rainvelle *et al.* (2002, 2004) conducted simulations as well as experiments on vanes thermal stresses and temperature profiles. The severe erosion of jet vanes has drawn the attention of a number of researchers. DeChamplain *et al.* (2002) attempted to experimentally quantify the erosion on vanes while Harrisson *et al.* (2003) examined the impact of jet vane erosion on TVC system efficiency. Danielson (1989) focused on the impact of propellant metal content on vane durability while Kumar *et al.* (2011) tested the use of composite materials in vanes. Structure reliability and failures of jet vane system were analyzed by Raouf, Pourtakdoust and Paghaleh (2018).

In the open literature, a number of studies were devoted to understanding the performance aspects of jet vane TVC system using experimental measurements and computational simulation techniques. Early studies (Harrisson *et al.*,2003, Giragosian 1981, Lauzon 1981) adopted the experimental approach. In his pioneering work, Giragosian (1981) measured the forces and rolling moments on a missile using a TVC including four vanes placed at the nozzle exit of a static test motor. Lauzon (1981) conducted a set of experiments to measure lift, drag, and control moment on a single vane

placed downstream the nozzle exit at various angles. The experiments of Harrisson *et al.* (2003) addressed the temporal profile of the lift on two opposite vanes placed outside the nozzle at deflection of 10º and 20º.

Roger *et al.* (1995) conducted CFD simulation study of a jet vane mounted at the exit of a rocket nozzle. The results were compared with those of a static hot fire test. The maximum vane deflection angle and the associated thrust losses were addressed. Rainvelle *et al.* conducted a series of numerical simulation validated with experimental measurements (2002, 2004). They examined a single vane placed outside the nozzle at zero deflection and its impact of the thrust-time profile of the engine. In the comprehensive numerical simulation study of Sung and Hwang (2004), two vanes placed at a fixed location in X-formation inside a shroud at the nozzle exit were examined in a half 3D domain. Simulations were validated with experimental measurements and the impact of vanes deflection of thrust losses and lateral force was examined. It was pointed out that the lateral force is due to three components as a result of pressure distributions on vanes, shroud inner walls and base. Murty and Chakraborty (2015) conducted a brief simulation study on a single vane placed outside the nozzle. The impact of engine total pressure and vane deflection on forces and moments acting on the vane was addressed. No validation for numerical simulations was reported.

Recently, a multi-disciplinary design of a single jet vane placed outside the nozzle was attempted by Çıtak *et al.* (2016) based on numerical simulations. The impact of vanes axial location was addressed by Kostic *et al.* (2017). The variation of axial and normal forces on a single vane placed at various locations and deflection angles inside a 2D nozzle was examined both experimentally and numerically. Finally, Söğütcü and Sümer (2019) examined numerically and experimentally the impact of vane deflection (up to 30 degrees) on temporal profiles of axial thrust and lateral force as well as drag on a single vane placed outside the nozzle.

Despite that previous studies have covered a variety of aspects of jet vane TVC, it is believed that the rich problem of jet vanes aerodynamics invokes more studies. For instance, the impact of jet vanes location was only addressed using a single vanes on a 2D nozzle (Kostic *et al.* 2017). However, the practical case in which four vanes are mounted in a shroud at the nozzle exit (as in Sung and Hwang 2004) was not clearly examined. In addition, the components of control force generated by the vanes were not thoroughly studied before and deserve deeper investigation. More importantly, the aspects of practical implementation of jet vanes TVC especially, the actuation moment and the overall functional efficiency of the system were not addressed in the open literature. It is also interesting to explore the three-dimensional flowfield downstream of the jet vane device at different vane locations and deflection angles.

In the present study, aerodynamic and performance features of an add-on jet vane TVC kit are numerically explored. The kit is composed of a cylindrical shroud with four inner vanes arranged in an X-formation to be fitted at the exit of a generic rocket nozzle. The location of vanes inside the shroud and their deflection angles are varied. The study goals are to address the impact of adding the kit and vanes arrangement on the lift and drag forces on the vanes, thrust losses and inclination, actuation moment and overall system efficiency, and flow field structure. The remainder of this paper is organized as follows. In the next section, the case study and methodology of tackling the problem in hand are explained. Following this, the main findings of the study are presented and discussed. Finally, the main conclusions are presented.

2. Add-on TVC kit

The case in concern is an add-on TVC kit composed of four jet vanes attached to a shroud. The

kit is sought to be attached to any rocket nozzle. Since the present work is more concerned with the design of the kit, a generic nozzle profile is adopted. Here, the nozzle profile examined by Pitz *et al*. (2011) is utilized having contraction and expansion area ratios of 11.3 and 7.4, respectively. The shroud is proposed as a cylindrical section of length equaling 0.54 D where D is the nozzle exit (shroud inner) diameter. The four jet vanes are evenly distributed circumferentially on the inner shroud surface in X-formation arrangement that easily yields more control force and provides roll control that stabilize missiles at launch (Sung and Hwang 2004). The geometry and dimensions of the jet vanes are adopted form the work of Giragosian (1981) that includes full details about vane geometry, dimensions, as well as full set of credible measurements. The vane has a double-wedge airfoil with blunted edges, aspect ratio of 0.66, thickness-to-chord ratio of 0.16 and is hinged at 35% chord where the thickness is maximum. The location of hinge point with respect to the cylindrical shroud upstream port is variable and is referred to hereafter as the *vane location*. A realization of the nozzle equipped with the TVC kit is illustrated in Fig. 1.

Thrust is produced by the nozzle as a reaction to the rate of change of momentum of the gas products as they exit the nozzle. The value of thrust is estimated by the equation (Sutton and Biblarz 2016)

$$F = \dot{m}W_e + S_{exit}P_{exit} = \dot{m}\left[W_e + \frac{S_{exit}P_{exit}}{\dot{m}}\right] = \dot{m}W_{eff} \tag{1}$$

where $\dot{m}$, W_e, P_{exit} are the gases mass flow rate, velocity, and gage pressure at the nozzle exit with an area S_{exit}, respectively. Clearly, adding the kit to the nozzle would have impact on the
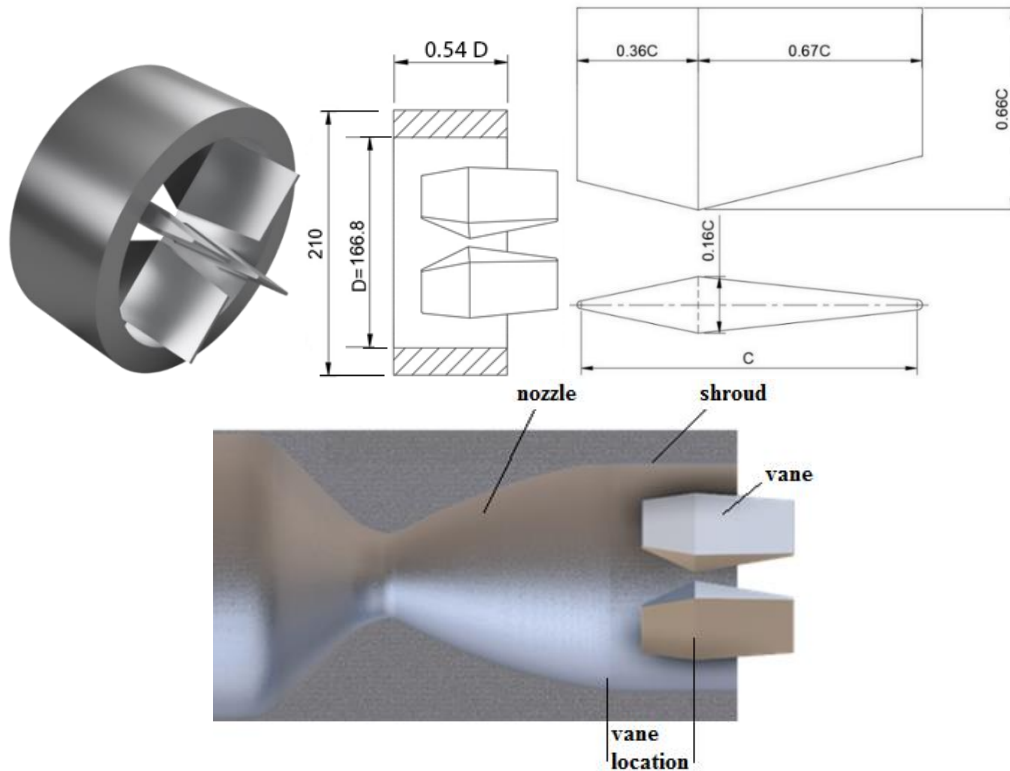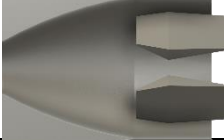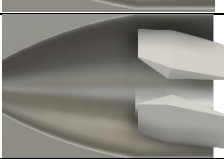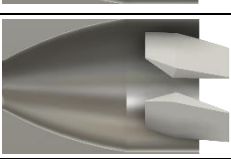

Fig. 1 Configuration of the proposed add-on TVC kit

Table 1 Plan and features for cases in concern in the study

| | | | Vane location | |
			At $0.24D$	At $0.36D$
Plain nozzle		√		
Nozzle+shroud only		√		
Nozzle+ TVC kit	Vane deflection	0º		
		5º		
		10º		
		15º		

values of exit area as well as the flow properties. The effective exhaust velocity, W_{eff}, of the gases can be viewed as the thrust per unit mass flow rate of the gases. Hence, it is adopted here as the measure of thrust produced by the nozzle with/without the kit attached. Due to interaction with the flow inside the nozzle, jet vanes are exposed to aerodynamic loads. Drag acts in the direction along the nozzle axis while lift is generated normal to the nozzle axis. Lift is the key output of the vanes. It is the main control force component used to generate the desired moment on the rocket.

The goal of the present study is to address the features associated with adding such TVC kit on the overall performance of the nozzle as a "thrust-generator". The impact of adding both the shroud and the vanes (at different vane locations) on the effective exhaust velocity of the gases for specific combustion chamber pressure is addressed. Two locations are considered here namely, at $0.24D$ and $0.36D$ from the shroud upstream port. In addition, the impact of vanes deflection angle at both locations on the aerodynamic loads on the vanes, nozzle effective exhaust velocity, control force value, and thrust deflection is investigated. Four different angles are considered namely, 0, 5, 10, and 15 degrees with respect to the shroud axis. Finally, the pattern and structure of the flow inside the nozzle and the kit are explored for the cases investigated. The cases to be examined are listed in the Table 1; illustrations for all cases with vanes are shown.

3. Numerical model and validation

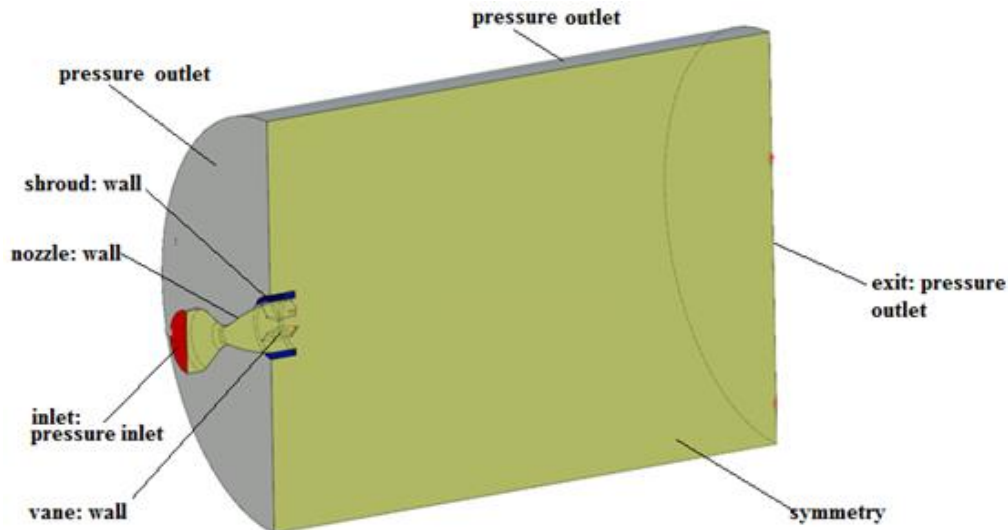The study is conducted by simulating the flow based on computational fluid dynamics (CFD)

Fig. 2 Outline and boundary definition of the computational domain

approach. A widely-used commercial CFD package is utilized (ANSYS Fluent 2012). Ten distinct numerical simulation cases are involved as marked in the table above. For each case, a 3D computational domain is constructed. Since the flow and domain are pitch-plane symmetric, only half of the full domain is considered. The general layout of the computational domains is illustrated in Fig. 2.

The domain extends in the radial and downstream directions are $8.1D$ and $12.69D$, respectively. At the nozzle inlet, a pressure inlet boundary is imposed with total and static pressures are equal to 31.3 bar such that flow inlet velocity is almost zero. This value corresponds to combustion chamber conditions in the work of Pitz *et al.* (2011). At the domain upstream, downstream, and lateral boundaries, pressure outlet boundary condition is implemented such that all properties are extrapolated from domain interior. All solid boundaries are defined as no-slip wall whereas symmetry boundary is defined at the pitch plane across the domain. In all cases, unstructured grids are implemented outside the boundary layers. Each case has a different gridding strategy. For the plain nozzle case, the grid is clustered downstream along the nozzle axis to capture the details of the jet structure while for the nozzle with shroud, grid is clustered in the vicinity of the nozzle exit. Finally, for the main cases of nozzle with TVC kit, grid is clustered in the nozzle and kit cavities as well as up to a distance downstream of the exit yielding relatively more cells. Samples of the grids are shown in Fig. 3 where the number of cells for each grid is also shown. Grid resolution in the kit cavity is shown separately.

Air as an ideal gas is adopted as the working fluid. The steady turbulent flow through the computational domain is solved using a second order scheme along with the Spalart-Allmaras one-equation turbulence model (Spalart and Allmaras 2002) that proved highly acceptable accuracy in similar high speed complex flows (Deck *et al.* 2002). The non-dimensional wall distance y+ was kept below 1 over vanes and shroud surfaces.

In order to assess the validity of the present CFD model in handling the problem in hand, two experiments from literature were numerically reproduced. The first experiment was conducted by Pitz *et al.* (2011) on a plain nozzle. The chamber stagnation pressure was 31.3 bar and the flow

(a) plain nozzle (cells count: 3,565,445)   (b) nozzle with shroud (cells count: 1,331,292)

(c) nozzle with TVC kit (cells count: 4,216,593)
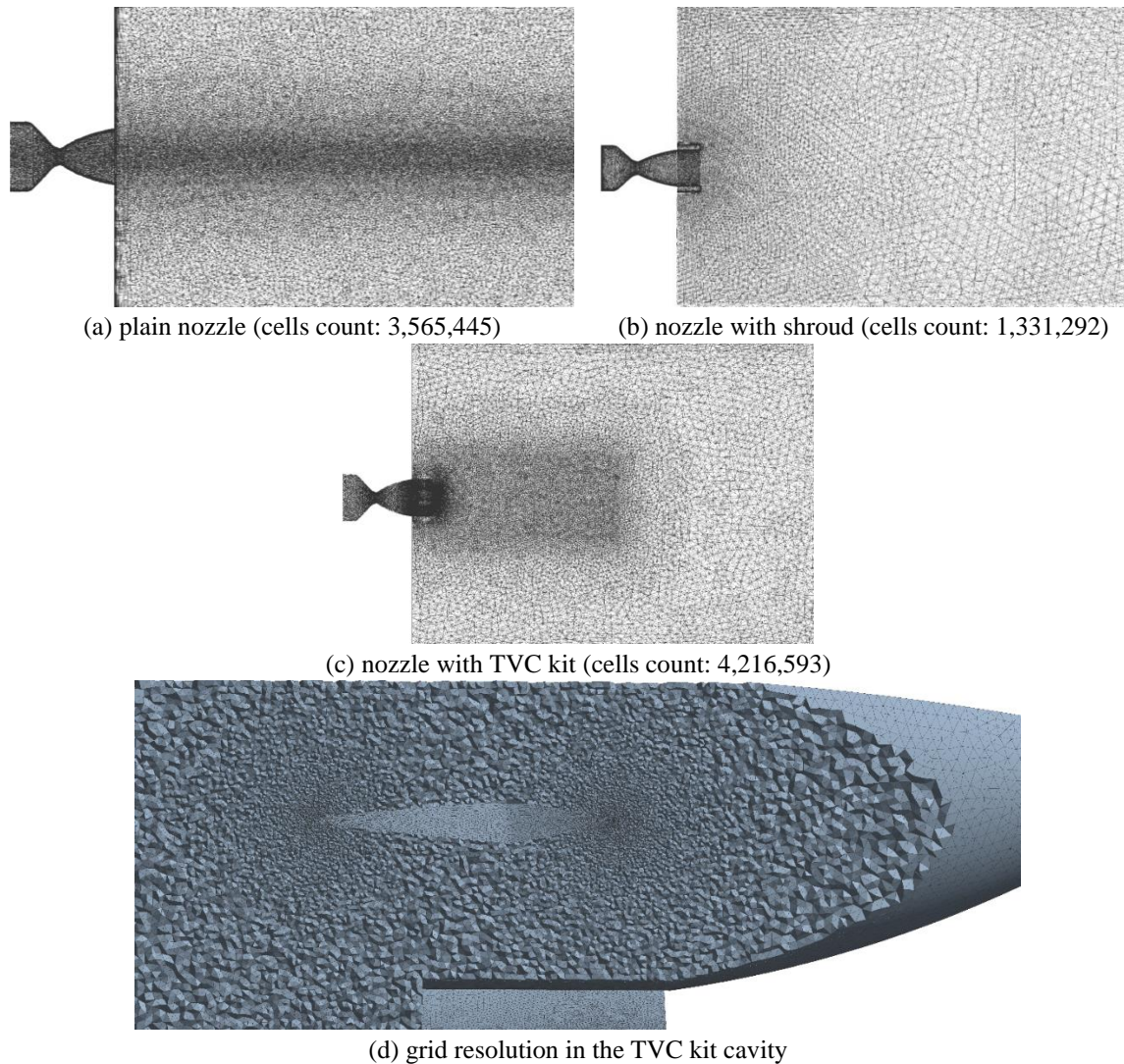
(d) grid resolution in the TVC kit cavity

Fig. 3 Discretized computational domains for sample cases

pressure at different locations along the nozzle wall was measured. A two-dimensional axis-symmetric model is developed for the reproduction of the experiment using the same CFD solver setup. The computational domain, Fig. , is discretized using a structured grid; a zoom-in at the nozzle is shown.

To simultaneously assess the spatial resolution quality, a grid independence check is conducted. Five grids with different resolutions, mesh 0 to mesh 04, are generated by successively reducing cell size by 50%. The total number of cells in the grids varied from 186100 to 81840 cells, respectively. It is found that the CFD model manages to predict the pressure profile along the nozzle wall with high accuracy for all grids. Fig.   compares the computed and measured pressure values where very good agreement between the experimental and numerical results can be shown. The settings of the grid with intermediate number of cells; 133225, are used is the following simulations.
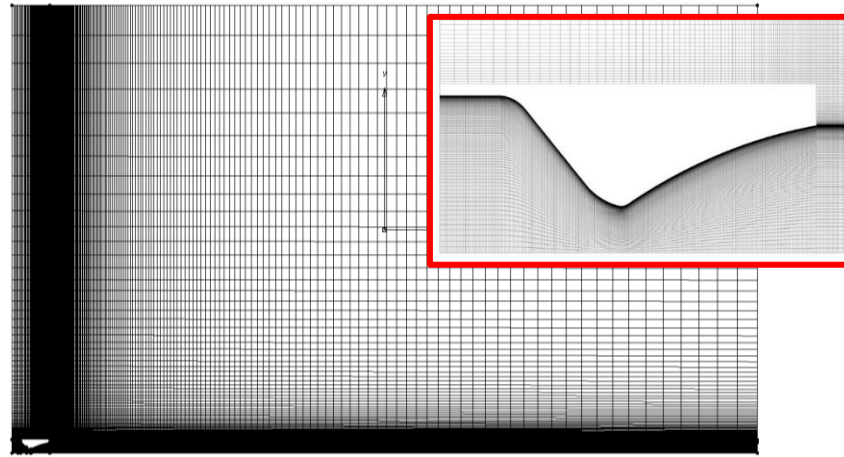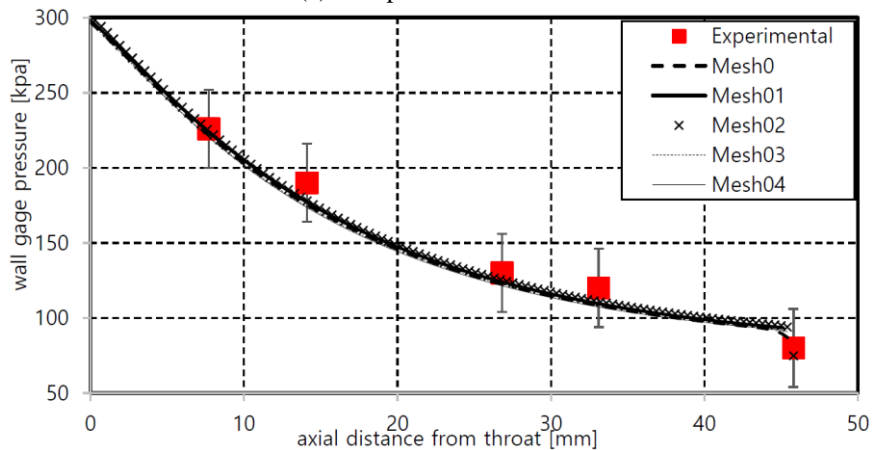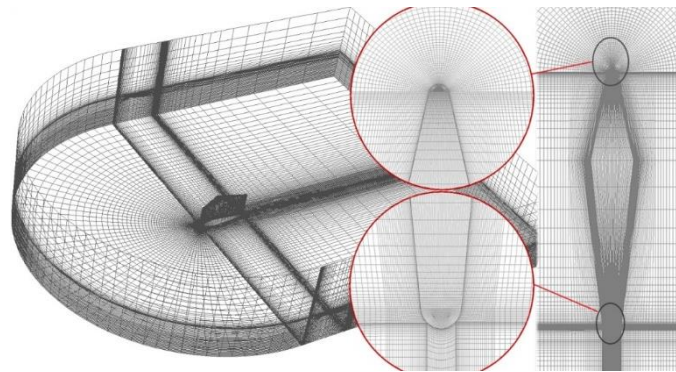
(a) Computational domain

(b) Computed vs. measured wall pressure profiles (Pitz *et al.*, 2011)

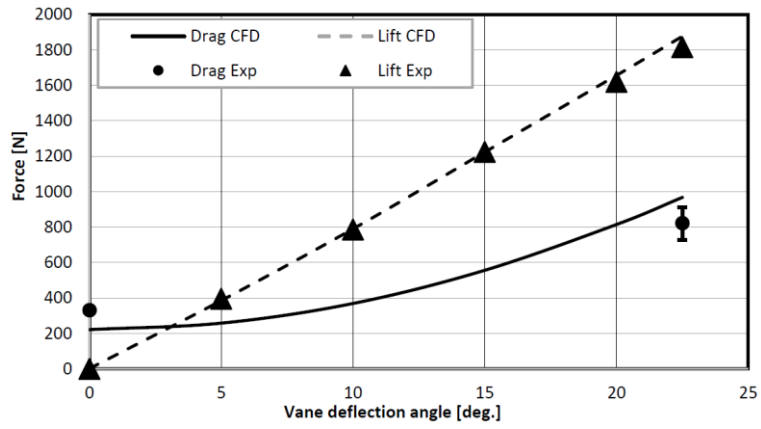Fig. 4 The plain nozzle validation case

The other validation case represents experiments conducted by Giragosian (1981) to measure the forces acting on a jet vane (the one adopted in the present work) at different deflection angles. In those experiments, the flow conditions corresponded to total pressure and Mach number of 20 bar and 3.4, respectively. The CFD model is implemented in the reproduction of Giragosian experiments. A three-dimensional computational domain is constructed and discretized into a multi-block structured grid including 2.1 million cells using the same settings for a grid-independent simulation. The discretized domain is illustrated in Fig. 5(a). The computed drag and lift forces acting on the vane are compared with those measured experimentally. The computed values are found in good agreement with their measured counterparts; Fig. 5(b).

4. Results and discussion

4.1 Impact of vane location and deflection on the jet structure
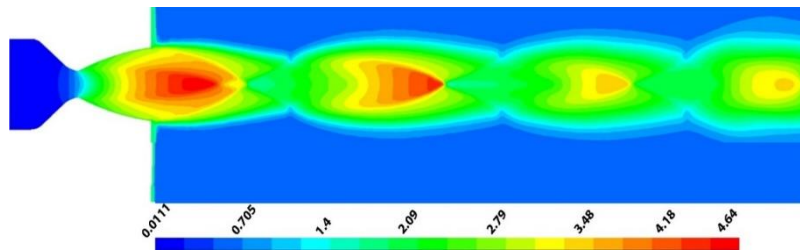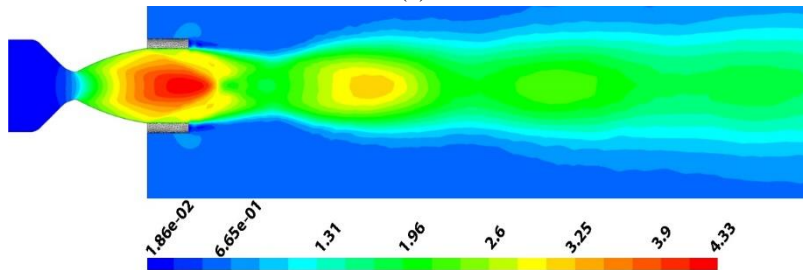
(a) Computational domain

(b) Computed vs. measured forces on vane (Giragosian, 1981)

Fig. 5 The computational domain for the vane validation case

(a)

(b)

Fig. 6 Jet flow Mach contours along and downstream of (a) the plain nozzle and (b) nozzle with Shroud

(a) 0° deflection

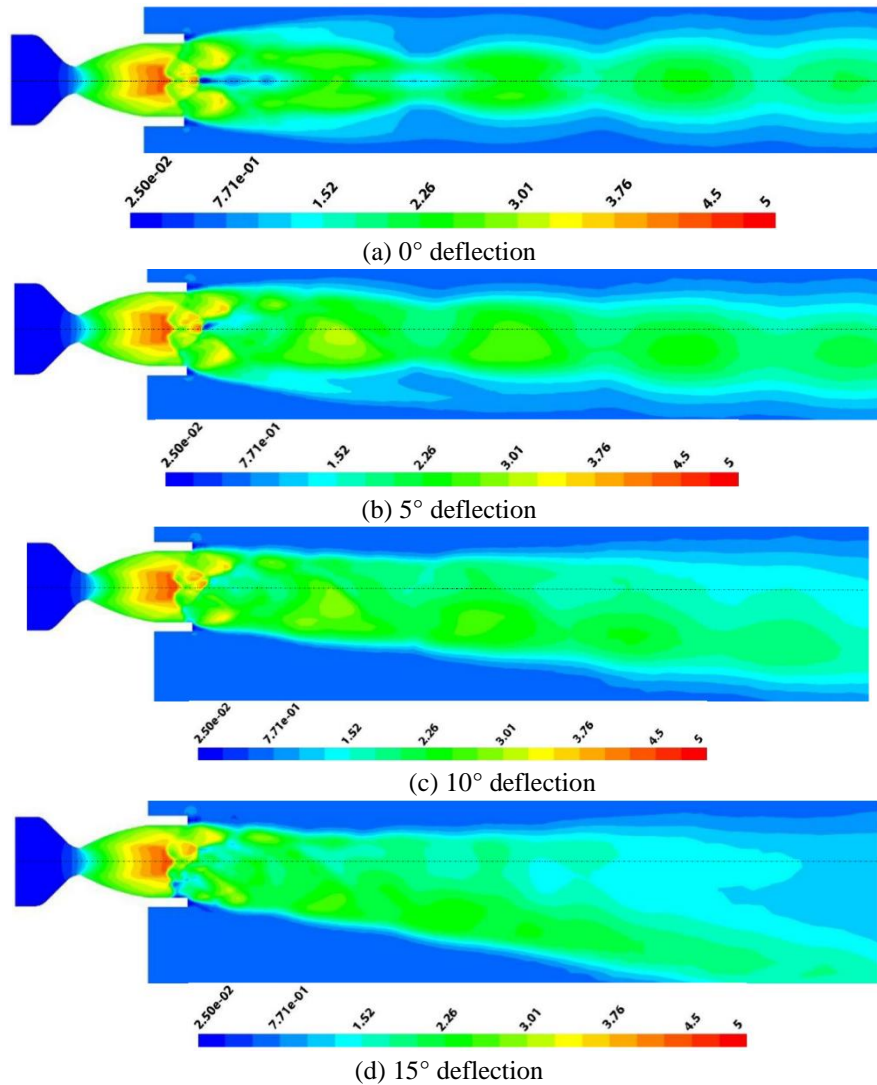(b) 5° deflection

(c) 10° deflection

(d) 15° deflection

Fig. 7 Jet flow Mach contours along and downstream the nozzle with TVC kit, vane location: 0.24D for different vane deflections

Fig. 6 shows the changes taking place in the structure of the jet flow along and downstream the nozzle with/without the shroud. The role of adding the vanes at 0.24D and 0.36D is illustrated in Figs. 7 and 8, respectively.

Closely examining the flow structure in Figs. 7 and 8 indicates that as the inclination angle increases, the jet gets more inclined with respect to the nozzle axis. The vanes location has the impact of increasing the inclination and distortion of the jet exiting the TVC kit. This is more clearly illustrated in Fig. 9 where the velocity contours over a plane normal to the nozzle axis at 1.5 m downstream of its exit are shown.

The increase in jet flow structure distortion with vane deflection angle is evident. The downward deflection of the jet significantly varies with the vane deflection angle while it is less dependent on

(a) 0° deflection

(b) 5° deflection

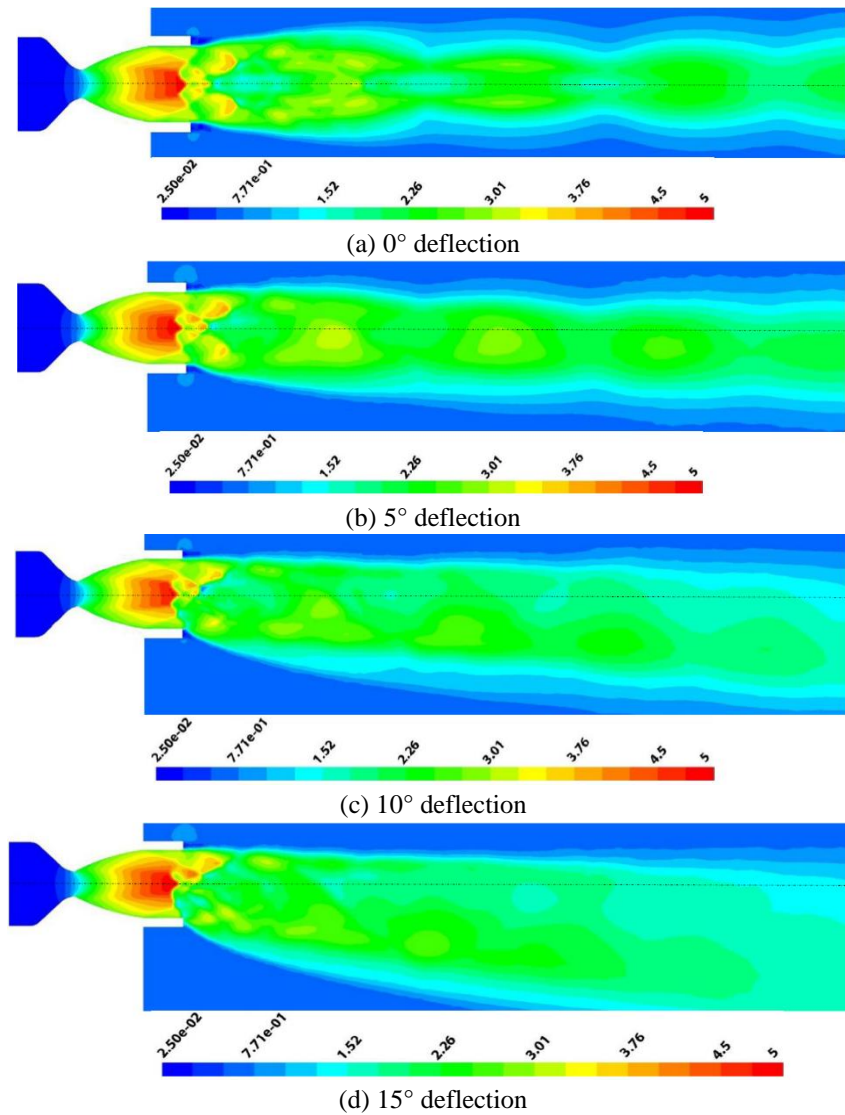(c) 10° deflection

(d) 15° deflection

Fig. 8 Jet flow Mach contours along and downstream the nozzle with TVC kit, vane location: 0.36D for different vane deflections

Table 2 Jet deflection angles for different TVC kit designs

		Vane deflection angle		
	Vane location	5°	10°	15°
Jet deflection angle, θ	0.24 D	1.9°	3.8°	6.1°
	0.36 D	2.1°	4.7°	7.23°

the vane location inside the shroud. The angle of jet deflection, θ, can be roughly inferred from the above figures using the simplified geometric relation shown in Fig. 9(e). Values of θ for different vane locations and deflections are listed in Table 2.

(a) 0° deflection (b) 5° deflection (c) 10° deflection (d) 15° deflection

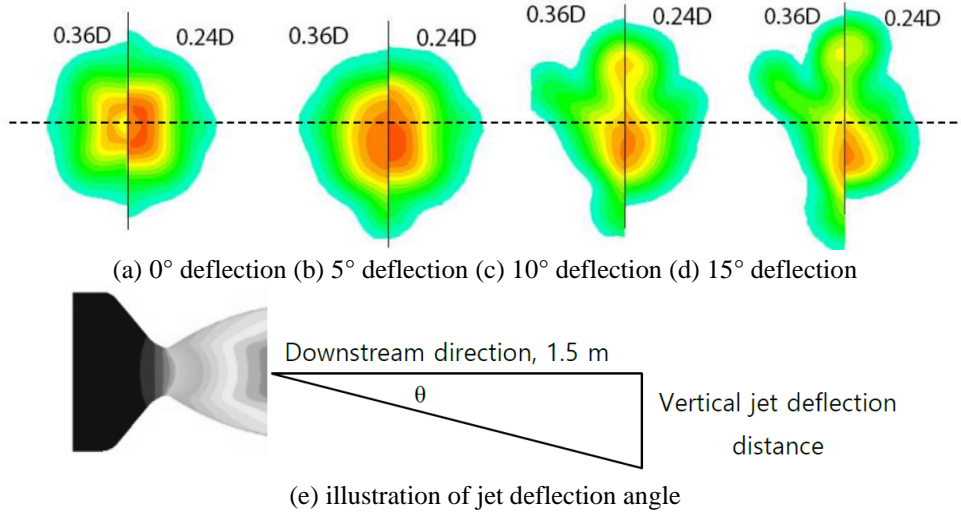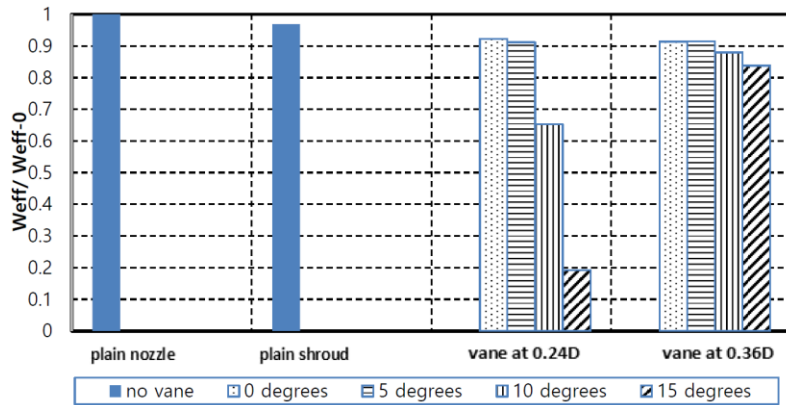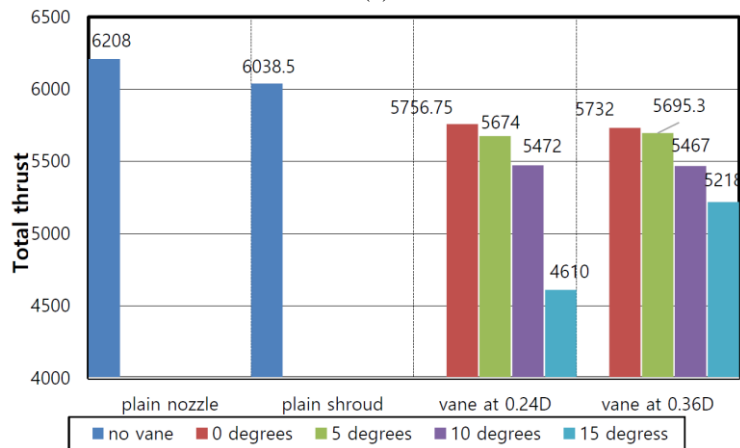(e) illustration of jet deflection angle

Fig. 9 Velocity contours 1.5 m downstream of the nozzle exit

(a)

(b)

Fig. 10 Variation of nozzle (a) effective exhaust velocity, and (b) total thrust with TVC kit design parameters
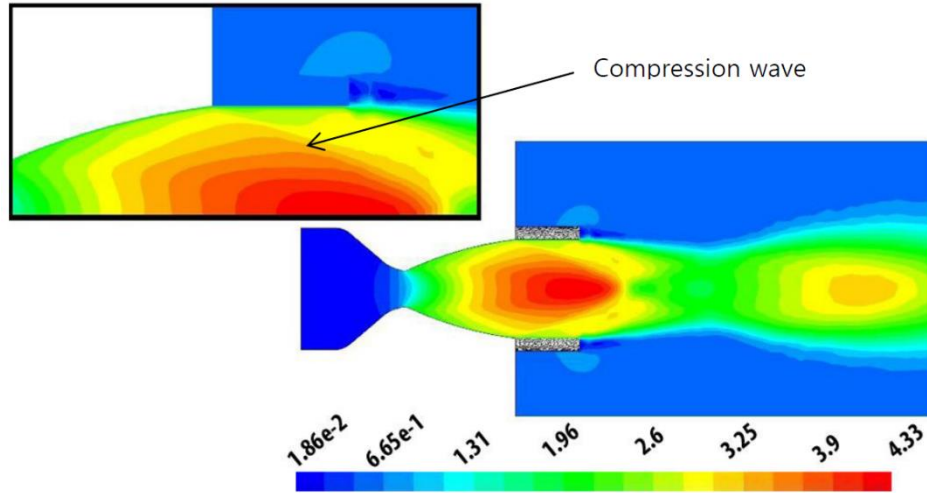
Fig. 11 Mach contours of flow through nozzle with plain shroud

4.2 Impact of vane location and deflection on the total thrust

Fig. 10 illustrates the variation of the average effective exhaust velocity and thrust of the nozzle upon adding the TVC kit. According to Eq. (1), thrust is calculated by adding the sum of $\dot{m}W_e$ to the surface integral of static pressure of the flow at the exit plane. The effective exhaust velocity is calculated as the surface integral of $(P_{exit}/\dot{m})$ over the nozzle exit plane. The values shown in the figures below are normalized with respect to those of the plain nozzle.

Fig. 10 indicates that adding the kit has a negative impact on thrust. A loss of about 2.7% in thrust is attained only due to the plain shroud with no vanes. This may be owed to the flow compression at the corner of the nozzle-shroud interface and (slightly) due to flow friction over the shroud surface. To illustrate this more clearly, the flow field is explored. Fig. 11 shows the Mach number contours of flow through the nozzle with plain shroud. It indicates that a compression wave is created at the nozzle-shroud junction. This wave, along with the additional friction along the added surface of the shroud may be the cause for the slight reduction in effective exhaust velocity and nozzle total thrust.

Back to Fig. 10, the thrust of the nozzle with the kit continues to decrease upon adding the vanes. With no vane deflection, an additional drop of 5% in total thrust that is almost insensitive to the vane location is attained. The losses in thrust increase monotonically with vanes deflection regardless of their location. The impact of vanes deflection is more severe if they are located closer to the nozzle throat and less pronounced as the vanes get closer to the shroud exit. This may be explained by the fact that the blockage of the flow passage caused by the vanes becomes less evident as the vanes location shifts downstream. The total nozzle thrust can lose as much as 25% of its value upon deflecting the jet vanes by 15°.

C. Variation of the forces acting on the vane

The variation of the forces acting on the jet vanes with their locations and deflection is illustrated in Fig. 12.

Fig. 12 shows that both lift and drag increase monotonically with the vane deflection angle. In addition, lift shows a nearly linear dependence with deflection. In contrast, the rise in drag shows
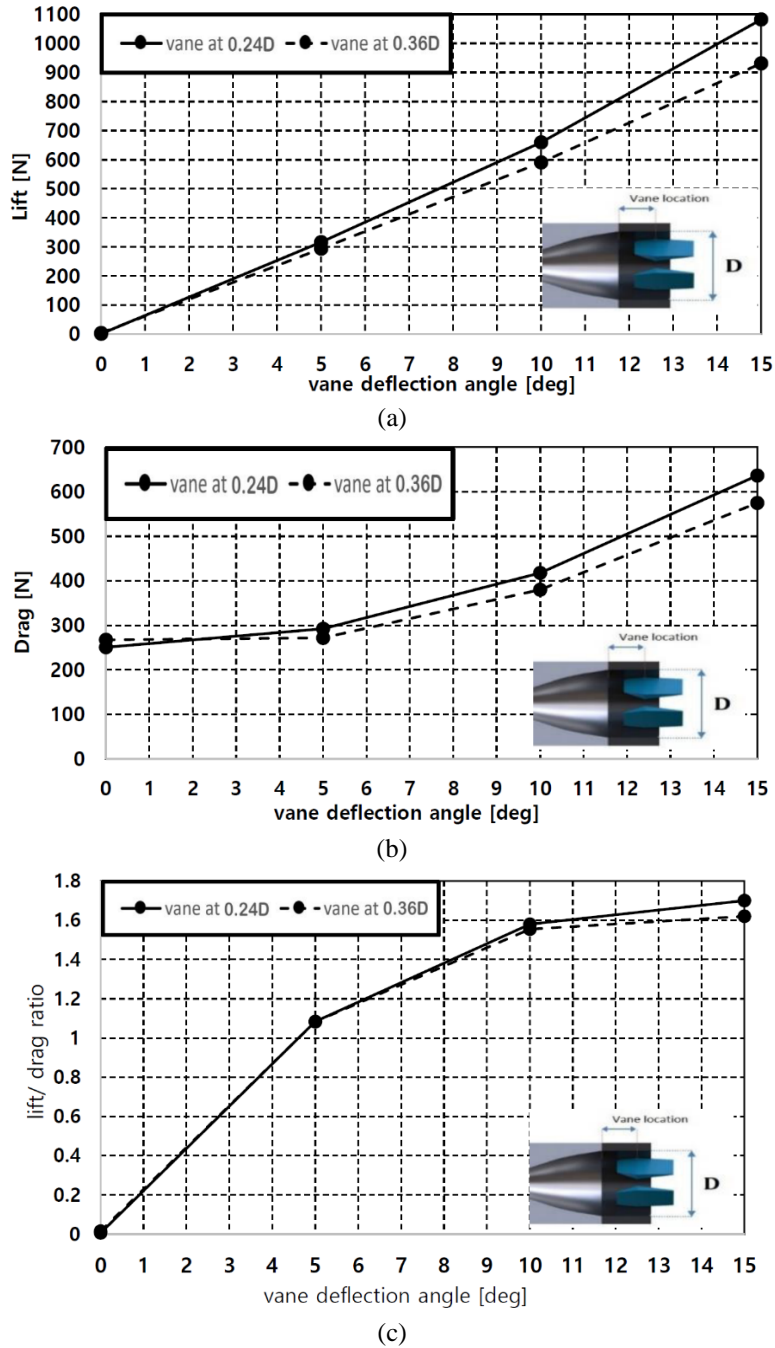
(a)

(b)

(c)

Fig. 12 Variation of (a) lift, (b) drag, and (c) aerodynamic efficiency of vanes with vane location and deflection

an increasing gradient with deflection angle. Overall, the aerodynamic efficiency, lift per drag, is higher at small deflection angles and deteriorates more rapidly as the deflection angle increases. At large deflection angles, the aerodynamic efficiency of the vane appears to reach a plateau profile
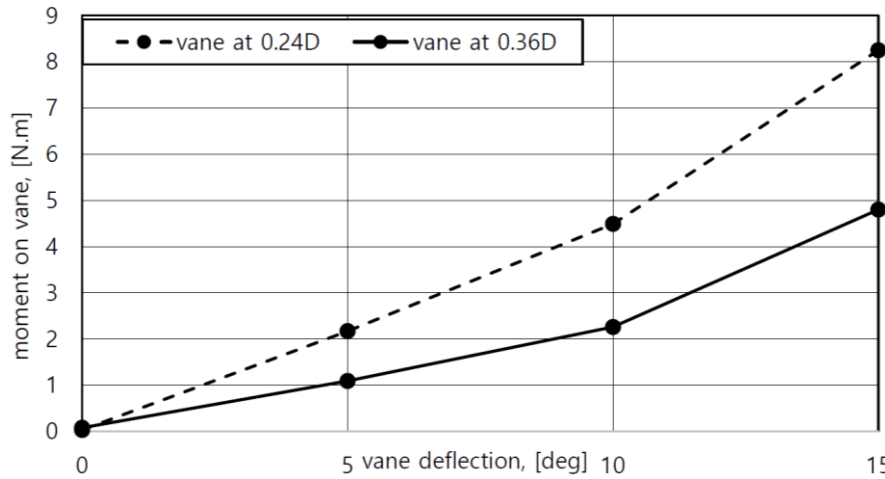
Fig. 13 Variation of aerodynamic moment on vane with vane location and deflection
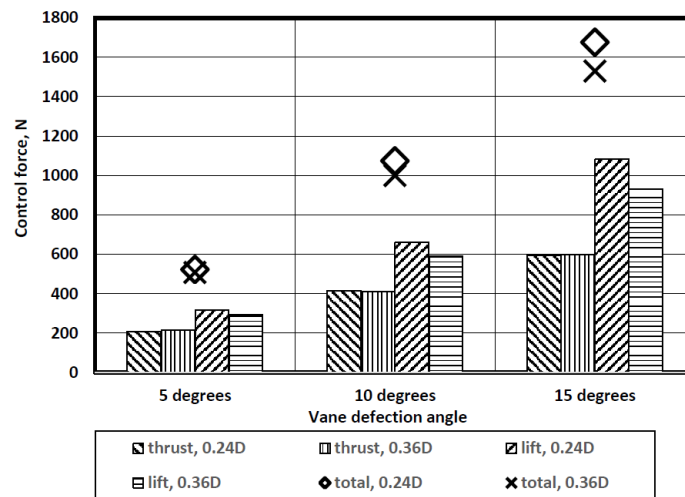

Fig. 14 Components and total control force for different TVC kit designs

with respect to variation of vane deflection angle.

The axial location of the vane inside the shroud appears to have a minor impact on its aerodynamic forces and efficiency of the vanes. Generally, shifting the vanes further downstream along the shroud has the role of reducing lift, drag, and aerodynamic efficiency of the vanes at all deflection angles. The role of vane location is more pronounced at small deflection angles.

Finally, Fig. 13 shows the impact of vane location and deflection angle of the aerodynamic moment acting on it around the hinge location. This is the moment that is to be applied to the vane by the control actuators. The relatively small values of moment may be owed to the small size of the vane and the low upstream total pressure. As shown in Fig. 13, the aerodynamic moment increases monotonically with deflection angle. Unlike in lift and drag, vane location has a clearer impact on aerodynamic moment. Placing the vane further downstream reduces the control demands in terms of actuation moment.
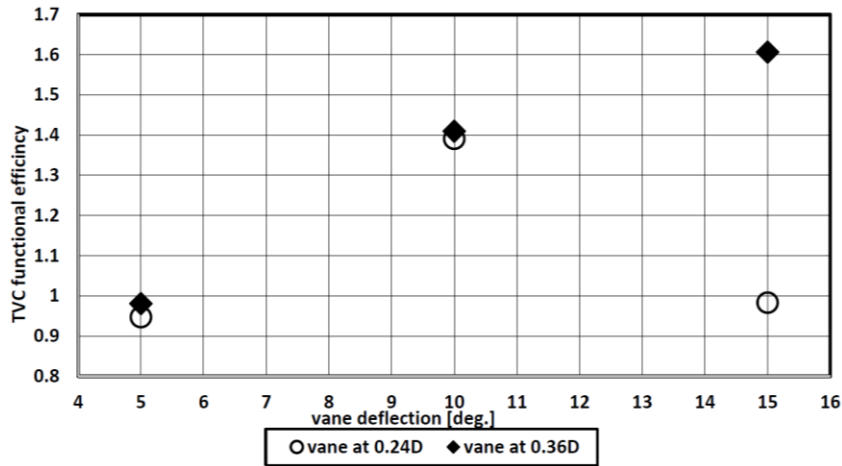
Fig. 15 Dependence of TVC kit efficiency on its design parameters

D. Impact of TVC kit design on the control force

Jet vane TVC generates a (lateral) control force that is the sum of two forces namely, lift on the vane and the reaction due to jet deflection. The authors argue here that these two components are distinct such that one is not a reaction to the other based on the following three aspects. Firstly, lift on vanes is physically transferred to the missile body through hinges causing an equal lateral control force that will be generated even if vanes are totally immersed inside the nozzle such that the exhaust jet is not deflected. Secondly, the change in jet direction is translated into another force that is equal to the lateral momentum of jet. This creates another different force that will be created even if no vanes are present. Finally, the two forces are in the same direction; e.g., a downward vane deflection yields a downward jet deflection. Hence, both the lift on vane and reaction due to jet deflection are in the same direction; upwards and are thus less likely to be an action and a reaction.

Lift on vanes has been presented earlier, Fig. 12, while reaction due to jet deflection can be easily obtained by calculating the lateral component of thrust, Eq. (1), at the nozzle exit surface, (Zivkovic 2016). Fig. 14 illustrates the two sources of control force, lift and thrust, and their sum for each of the TVC kit designs in concern.

It can be inferred from Fig. 14 that, both components of control force increase monotonically with vane deflection. In addition, lift and thrust control force components have almost equal contribution in the total control force; the former is slightly dominant since it constitutes 58%: 68% of the total. This dominance is slightly more evident for closer hinge locations of the vane and increases slightly with vane deflection angle. Shifting the vane hinge location further downstream reduces the lift component of the control force. This is more evident as the vane deflection angle increases and has been addressed before in Fig. 10. However, shifting the vanes location downstream has a positive impact on the thrust component of total control force; such impact increases marginally with vane deflection angle. Overall, the total control force is almost independent of vane location for the range of deflection angles investigated here. As shown in Fig. 14, the two control force components are not equal and even follow different trends in response to vane location. This confirms the argument proposed by the authors that these two components are not in action-reaction relation.

Finally, the impact of jet vane TVC design parameters on the overall functional efficiency of the

TVC kit is addressed. The efficiency here is defined as the ratio between the gains and losses. Gains are the total control force while losses are the losses in the total thrust of the nozzle upon attaching the TVC kit. Fig. 15 illustrates this dependence.

The gains and losses are almost equal at the lowest vane deflection angle examined. Increasing the vane deflection enhances the efficiency especially if the vane is located closer to the kit exit. If the vanes are hinged close to the nozzle exit, the efficiency reaches a maximum at moderate deflection angles and deteriorates by further increasing the deflection.

5. Conclusions

The design of an add-on jet vane kit to introduce the control features to plain nozzles is examined in the present study. The kit has the form of a cylindrical shroud with four vanes distributed evenly in x-formation. The study aimed to investigate the impact of vanes location in the shroud and deflection with respect to the nozzle axis. Focus was made on thrust losses, control force value, jet inclination, TVC kit efficiency, and flow structure. Numerical simulation using CFD techniques was implemented in the study. The main conclusions of the present study are as follows. Lift is more sensitive to vanes deflection angle rather than their location. In addition, the aerodynamic efficiency of the vanes diminishes at higher deflection angles. It is also found that thrust losses due to vanes deflection are more severe if their location is shifted further upstream. The Jet becomes more inclined and distorted as vanes inclination increases and location shifts further downstream. Finally, the results indicate that the TVC kit design incorporates a tradeoff between the value of control force generated by the vanes and the net value of axial thrust. Based on the present results, it may be recommended that the vanes be located further downstream of the nozzle.

More vane locations should be considered to confirm the findings of the present research. Moreover, the present simulations were conducted with air as the working gas. It is thus recommended to investigate the impact of real working gas on jet vane TVC kit operation.

References

ANSYS (2012), FLUENT User's Guide, ANSYS Inc.

BAE Systems (2018), APKWS Laser-Guided Rocket, https://www.baesystems.com/en/product/apkws-laser-guided-rocket.

Branislav, J., Momcilo, M. and Zoran, S. (1987), "Pressure distribution in rocket nozzle with mechanical system for TVC", *23rd Joint Propulsion Conference*, California, July. https://doi.org/10.2514/6.1987-1824.

Chandra Murty, M.S.R. and Chakraborty, D. (2015), "Numerical characterisation of jet-vane based thrust vector control systems", *Defence Sci. J.*, **65**(4), 261-264. https://doi.org/10.14429/dsj.65.7960.

Çıtak, C., Akdemir, M. and Yumuşak, M. (2016), "Multidisciplinary, multiobjective analysis and optimization for the design of missile jet vane", *17th AIAA/ISSMO Multidisciplinary Analysis and Optimization Conference*, Washington DC, June. https://doi.org/10.2514/6.2016-3832.

Danielson, A. (1990) "Inverse heat transfer studies and the effects of propellant aluminum on tvc jet vane heating and erosion", *26th Joint Propulsion Conference*, Florida, July. https://doi.org/10.2514/6.1990-1860.

Danielson, R.B. and Dillinger, A.O. (1989), "Investigation of thrust vector control for high-alpha pitchover", *ADP005875*, Naval Weapons Center, China Lake, CA.

Davidović, N., Miloš, P., Jojić, B. and Miloš, M. (2015), "Contribution to research of spoiler and dome deflector TVC systems in rocket propulsion", *Technical Gazette*, **22**(4), 907-905.

https://doi.org/10.17559/TV-20140621063849.

de Champlain, A., Harrisson, V., Kretschmer, D., Farinaccio, R. and Stowe, R. (2002), "Optical technique to quantify erosion on jet vanes for thrust vector control", *38th AIAA/ASME/SAE/ASEE Joint Propulsion Conference & Exhibit*, Indiana, July. https://doi.org/10.2514/6.2002-4190.

Deck, S., Duveau, P., d'Espiney, P. and Guillen, P. (2002), "Development and application of spalart-allmaras one equation turbulence model to three-dimensional supersonic complex configurations", *Aerosp. Sci. Technol.*, **6**, 171-183. https://doi.org/10.1016/S1270-9638(02)01148-3.

Facciano, A.B., Seybold, K.G., Westberry-Kutz, T.L. and Widmer, D.O. (2002), "Evolved seasparrow missile jet vane control system prototype hardware development", *J. Spacecraft Rocket.*, **39**(4), 522-531. https://doi.org/10.2514/2.3865.

Fuente, M. and Thirkill, J. (1964), "Evaluation of TVC systems for solid-propellant motor application", *Solid Propellant Rocket Conference*, January. https://doi.org/10.2514/6.1964-159.

Giragosian, P. (1981), "Theoretical and experimental aerodynamic correlation of jet vane control effectiveness", *7th Atmospheric Flight Mechanics Conference*, New Mexico, August. https://doi.org/10.2514/6.1981-1897.

Harrisson, V., deChamplain, A., Kretschmer, D., Farinaccio, R. and Stowe, R. (2003), "Force measurements evaluating erosion effects on jet vanes for a thrust vector control system", *39th AIAA/ASME/SAE/ASEE Joint Propulsion Conference and Exhibit*, Alabama, July. https://doi.org/10.2514/6.2003-5237.

Hunter, C.A. and Deere, K.A. (1999), "Computational investigation of fluidic counterflow thrust vectoring", *35th Joint Propulsion Conference and Exhibit*, California, June, https://doi.org/10.2514/6.1999-2669.

Kostic, O., Stefanovic, Z. and Kostic, I. (2017), "Comparative CFD analyses of a 2D supersonic nozzle flow with jet tab and jet vane", *Technical Gazette*, **24**(5), 1335-1344. https://doi.org/10.17559/TV-20160208145336.

Kumar, S., Kumar, A., Sampath, K., Bhanu Prasad, V.V., Chaudry, J.C., Gupta, A.K. and Rohini Devi, G. (2011), "Fabrication and erosion studies of C-SiC composite jet vanes in solid rocket motor exhaust", *J. Eur. Ceram. Soc.*, **31**(13), 2425-2431. https://doi.org/10.1016/j.jeurceramsoc.2011.06.007.

Lauzon, M. (1990), "5DOF dynamic loads on a jet vane", *26th Joint Propulsion Conference*, Florida, July. https://doi.org/10.2514/6.1990-2382.

Loyd, R. and Thorp, G.P. (1978), "A review of thrust vector control systems for tactical missiles", *14th Joint Propulsion Conference*, Nevada, July. https://doi.org/10.2514/6.1978-1071.

Nauparac, D.B., Pršić, D.H., Miloš, M.V. and Todić, I.S. (2015), "Different modeling technologies of hydraulic load simulator for thrust vector control actuator", *Technical Gazette*, **22**(3), 599-606. https://doi.org/10.17559/TV-20140621063240.

Pitz, R., Ramsey, M., Anderson, W., Jenkins, T., Matsutomi, Y. and Yoon, C. (2011), "Experimental velocity profiles in the cap shock pattern of a thrust optimized rocket nozzle", *49th AIAA Aerospace Sciences Meeting*, Florida, January. https://doi.org/10.2514/6.2011-1167.

Rahaim, C., Cavalleri, R., McCarthy, J. and Kassab, A. (2006), "Jet vane thrust vector control - A design effort", *32nd Joint Propulsion Conference and Exhibit*, Florida, July. https://doi.org/10.2514/6.1996-2904.

Rainville, P.A., de Champlain, A. and Kretschmer, D. (2002), "CFD validation with measured temperatures and forces for thrust vector control", *38th AIAA/ASME/SAE/ASEE Joint Propulsion Conference & Exhibit*, Indiana, July. https://doi.org/10.2514/6.2002-4192.

Rainville, P.A., deChamplain, A., Kretschmer, D., Farinaccio, R. and Stowe, R. (2004), "Unsteady CFD calculation for validation of a multi-vane thrust vector control system", *40th AIAA/ASME/SAE/ASEE Joint Propulsion Conference and Exhibit*, Florida, July. https://doi.org/10.2514/6.2004-3384.

Raouf, N., Pourtakdoust, S.H. and Paghaleh, S.S. (2018), "Reliability and failure analysis of jet vane TVC system", *J. Fail. Anal. Preven.*, **18**, 1635-1642. https://doi.org/10.1007/s11668-018-0563-9.

Roger, R., Chan, S. and Hunley, J. (1995), "CFD analysis for the lift and drag on a fin/mount used as a jet vane TVC for boost control", *33rd Aerospace Sciences Meeting and Exhibit*, Nevada, January. https://doi.org/10.2514/6.1995-83.

Söğütcü, B. and Sümer, B. (2019), "Experimental and numerical investigation of a jet vane of thrust vector control system", *AIAA Propulsion and Energy Forum*, Indiana, August. https://doi.org/10.2514/6.2019-

3880.

Spalart, P.R. and Allmaras, S.R. (1992), "A one equation turbulence model for aerodynamic flows", *30th Aerospace Sciences Meeting and Exhibit*, Nevada, January. https://doi.org/10.2514/6.1992-439.

Sung, H. and Hwang, Y. (2004), "Thrust-vector characteristics of jet vanes arranged in an X-formation within a shroud", *J. Propuls. Power*, **20**(3), 501-508. https://doi.org/10.2514/1.10381.

Sutton, G. and Biblarz, O. (2016), *Rocket Propulsion Elements*, John Wiley and Sons.

Tekin, R., Atesoglu, Ö. and Leblebicioglu, K. (2010), "Modeling and vertical launch analysis of an aero- and thrust vector controlled surface to air missile", *AIAA Atmospheric Flight Mechanics Conference*, Ontario, August. https://doi.org/10.2514/6.2010-7639.

Yu, M.S., Cho, H.H., Hwang, G.Y. and Bae, J.C. (2004a), "A study on a surface ablation of the jet vane system in a rocket nozzle", *37th AIAA Thermophysics Conference*, Oregon, July. https://doi.org/10.2514/6.2004-2276.

Yu, M.S., Cho, H.H., Hwang, K.Y. and Bae, J.C. (2006), "Hybrid method for jet vane thermal analysis in supersonic nozzle flow", *J. Thermophys Heat Transf.*, **20**(3), 614-617. https://doi.org/10.2514/1.17675.

Yu, M.S., Lee, J.W., Cho, H.H., Hwang, K.Y. and Bae, J.C. (2004b), "Numerical study on a thermal response of the jet vane system in a rocket nozzle", *42nd AIAA Aerospace Sciences Meeting and Exhibit*, Nevada, January. https://doi.org/10.2514/6.2004-997.

Zivkovic, S., Milinovic, M., Gligorijevic, N. and Pavic, M. (2016), "Experimental research and numerical simulations of thrust vector control nozzle flow", *Aeronaut. J.*, **120**(1229), 1153-1174. https://doi.org/10.1017/aer.2016.48.

GY